Disaster Risk Reduction Strategies for Pluvial & Fluvial Flood Resilience in Chennai city

M. Raja Kathiravan, Saikat K. Paul,

Department of Architecture and Regional Planning, Indian Institute of Technology,

Kharagpur, West Bengal, India

Abstract

Due to rapid urbanization and industrialization, modifications in land use pattern has brought about irreversible anthropogenic aggravations to the hydrological forms. This can be attributed to the impervious land surfaces in the urban area which increases the runoff component. The increased runoff along with diminishing percolation and reduction in the time of concentration influences the hydrological cycle thereby increasing the hazard of urban flooding in cities. Further, changes in the global climate pattern and local extreme weather events (pluvial patterns) exacerbates the problem of urban flooding which is being experienced throughout the world. Invincible vagaries of nature impel one to essentially address complications vis-à-vis urbanization (Urban sprawl) and land management. This study analyses the rainfall trends, watershed behaviour, characteristics of land cover, drainage pattern that stimulated the occurrence of flood events in the Adyar basin, Chennai, specifically the 2015 event. The entire process of flood stimulation has been carried out through computer-based modeling using GIS, hydrology and hydraulic tools. Key findings were made by interchanging the value of the parameters (rainfall and reservoir data) between 2005 and 2015 CN grid (combination of Land cover class and Hydrological soil group) to understand the impact of the land cover change in the ten years' time frame and to assess the management issue of the reservoir. Flood inundation map was generated in HEC-RAS environment with the knowledge of discharge data, versus time and characteristic parameters of the river. This helped in identification of risk-prone areas and future scenarios for 2035 were generated taking into cognition the demographic and physical growth of the city to predict the consequence of flood in the Adyar basin, Chennai. Further sustainable mitigation and disaster risk reduction strategies using both engineering and non-engineering measures were formulated towards building resilience to such pluvial events in Chennai as a consequence of global climate change. This research paves the way for better Urban Land Management practices that would make the city of Chennai resilient to both pluvial and fluvial flood events.

1. INTRODUCTION

Flood events have been consistently causing significant damage to life and property throughout the world. In the most recent decade of the twentieth-century flood accounted for around 12% of all deaths from catastrophic events, accounting for nearly 93,000 fatalities (Hannah Ritchie and Max Roser, 2017). The flood may also prompt other physical as well as psychological impacts like emotional trauma, fear of economic costs of clean-up, overhaul and reconditioning, etc. (Ohl & Tapsell, 2000). Asia alone accounts for a major share (70%) of the world's flood events. Average annual economic loss due to floods over the past decades is estimated to be 15 billion USD, with infrastructure loss solely accounting for 12 billion USD. Therefore, it proves to be an issue of immediate concern that the Governments across the world must address.

A flood is defined as "an impermanent state of complete or partial inundation on the general dry regions, due to the spillover of inland or tidal surge from the uncommon and quick accumulation or overflow of surface water from several sources" ("UN-SPIDER Knowledge Portal," n.d.). It is characterized by the greater flow of water over the levels of waterways, lakes, ponds, stores and other such water bodies, whereby water emerges outside of the water body's territory. Flooding likewise happens when the ocean level reaches above seaside land because of the tidal sea or ocean surges or excessive rainfall. In numerous states and nations, the surge is the most event that creates an impact on the social and financial existence of the populace (Smith, K., & Ward, 1998). Though floods affect various sections of the society impartially, the highly affected among them are the poor, who are left with dwelling in zones that are at higher risk of hazardous and catastrophic events (Price & Vojinovic, n.d.).

Floods result from a multitude of complex factors (urban heat effect, El-Niño, land cover change, etc.) at both urban and global levels. Addressing each of these causes only will resolve the problems rather than mere redressal of urban-level issues in completely controlling the floods. However, considering the limited data available, time, monetary and execution requirements, the investigation zone is limited to urban-level issues, which need immediate attention. Conventional engineering and non-engineering measures play vital roles in achieving effective mitigation of the damages caused by the floods in urban level. Delineation of flood risk maps to evaluate the urban area and bringing in land use changes are some factors that impart significance to the non-engineering measures. These address issues at their root but are tedious. On the contrary, engineering measures serve as quick-fixes but they may fail to deliver permanent solutions. These facts thus deem non-engineering measures as potentially sustainable. In this investigation, both the measures are utilized; however, greater preference is given to the non-engineering measures (Wiitala, Sommerville, Jetter, & Pennsylvania., 1961).

Forecasting hydrologic events using computer simulation tools have helped researchers and engineers in determining the extent of flood hazard and additionally with flood appraisals. Flood simulation and hazard assessment models include the following steps:

1) Hydrologic model: compute the relationship between rainfall and runoff in a given time frame from historic events.

2) Hydraulic model: courses the excess water through the river to decide water surface profiles at particular areas throughout the river network

3) Locating the floodplain and understanding the existing or future scenarios, and

4) The geospatial information is derived for the benefit of further studies or models (Snead, 2000).

The portrayal of the whole flooding event in simpler and visualizable format through these modeling is the key to analyze this hazard. GIS and other modeling software are pivotal to the above-mentioned process.

The main aim of the research is to measure the floodwater, create hydrograph, generate past and future scenarios with the procured and processed data, to explore the possibility of recharging the aquifer using portion of ensuing flood and to explore sustainable risk reduction strategies. Here, Adyar River, Chennai was chosen as the study area for the above analytical study.

1.1. Problem definition

Substantial precipitation occurred in two stages in Chennai from the month of November to December 2015. While Chennai was recouping from the first flood event, the city was struck by a second flood event of higher magnitude. This resulted in a devastating flood in Chennai and other coastal districts of Tamil Nadu. The flood caused losses estimated to be around ₹ 9,800 crores by the Government authorities.

2. STUDY AREA

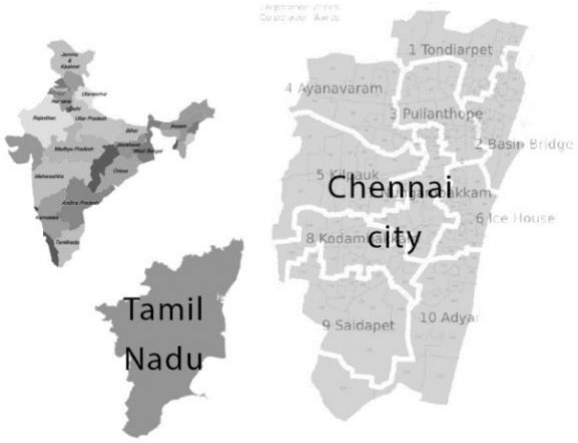

Figure 1: Location of Chennai city

Chennai is the fourth largest metropolitan city in India as per population. It is the capital of Tamil Nadu and is the nodal point for industries, business and functions as an administrative and financial hub in the region. It stands third in terms of GDP contribution to India after Delhi and Mumbai. Figure 1, shows the location of Chennai. The latitude, longitude, and elevation of Chennai are 13.067439, 80.237617, 13m MSL respectively. Chennai city is bounded by Valluvar in the north; Siruseri in the south; the Bay of Bengal in the east and Avadi in the west.

2.1. History of Chennai floods

Chennai city and its environs are flat with contours ranging from 2m to 10m above MSL, with very few separated hillocks in the south-west close to St. Thomas Mount, Pallavaram and Tambaram. The two rivers Adyar and Cooum running in the central and southern part of the city respectively have been causing flood in this region.

Table 1: List of cyclones that struck Chennai (from 2015)

Name	Lowest Pressure (mbar)	Year	Winds (km/hr)
Fanoos	998	2005	85
Nisha	996	2008	85
Jal	988	2010	100
Thane	972	2011	140
Nilam	992	2012	85
Madi	986	2013	120

Deep Depression (BOB 03)	-	2015	55
Roanu	983	2016	85
Kyant	997	2016	85
Nada	1000	2016	75
Vardah	982	2016	130
Ockhi	975	2017	155

River Cooum gathers surplus water from around 75 tanks in its catchment inside Chennai Metropolitan Area (CMA) and Adyar river gathers surplus from around 450 tanks in its catchment, in addition to the overflows from the huge Chembarambakkam Tank. Chennai is an example of the disastrous event of flooding which occurred during November to December, 2015, because of the overwhelming precipitation related to depressions and cyclones. It is one of the cataclysmic flood events in the sequence of 1976, 1985, 1996, 1998, 2005, 2008, 2010 but stood distinct in creating substantial damages. Table 1 shows the details of the cyclone that struck Chennai in the past.

2.2. Adyar river

Adyar river originates from Aadhanur lake and Chembarambakkam lake in Kanchipuram region. The length of the waterway is 42 km and the slope of the river ranges from 1/1000 to 1/2000 covering the Chennai and Kanchipuram districts. The waterway joins the Bay of Bengal close to Besant Nagar. It has almost 23 drains/canals draining into the river directly with 28 bridges over the main stream up to Aadhanur lake. Currently, the waterway has a check dam, and an embankment in Nandambakkam and Kundrathur respectively. It is a more extensive waterway when contrasted with Cooum with more prominent depth near the mouth. The average annual runoff in the river is 61.42 MCM. Total water source potential in the basin is 474 MCM, the gross demand for the basin is 1323 MCM and total water deficit is 849 MCM. It has nearly 150 tanks in the basin, which irrigates an area of 18453 Ha (LKS Pvt. India, 2012).

3. METHODOLOGY

The methodology adopted is explained in Figure 2. The methodology mainly comprises of rainfall analysis, hydrology and hydraulic modeling.

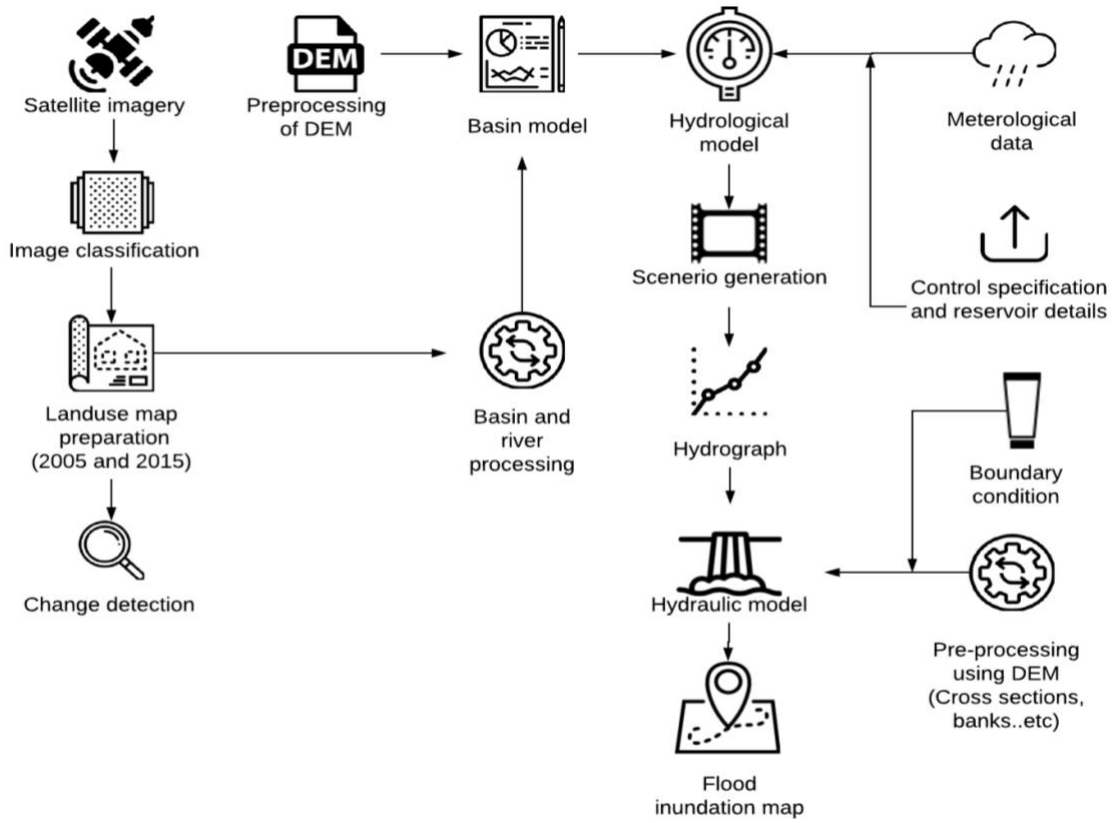

Figure 2: General flowchart of the methodology

Source: (Hernandez & Zhang, n.d.) &(Curebal, Efe, Ozdemir, Soykan, & Sönmez, 2016)

3.1. Rainfall analysis

The total precipitation in a given period in an area is exceedingly different from one year to another. The fluctuation relies upon the type of climate and the length of the considered period. As a rule, it can be expressed that the drier the climate, the higher the fluctuation of precipitation in time. A similar rule holds for the length of the period: the shorter the period, the higher the yearly inconstancy of precipitation in that period (Haan, 1986).

Probability of exceedance (P_X): The probability of exceedance refers to the probability of the occurrence of a precipitation depth more prominent than some given value X_P. The probability of exceedance (P_X) is communicated as a portion (on a scale extending from zero to one) or as a percentage chance with a scale going from 0 to 100. If the evaluations refer to the precipitation depth that can be expected or maybe surpassed in a year during the reference time period, then it can be communicated as a set number of years out of an aggregate number of years.

Rainfall data of Chennai from 1901 to 2015 is used to evaluate the probability of exceedance (CDF) using the California Method (Works, 1923) which uses, the normal distribution.

$$\text{Probability of exceedance} = \frac{r}{n}\ x\ 100\ \%$$

Where 'r' is the ranked number and 'n' is the total number of observations.

Calculation for Probability of exceedance has been carried out in the study with the help of software named 'RAINBOW' developed by K.U.Leuven University-IUPWARE.

Return period (T_X): The return period (likewise called the recurrence interval) T_X is the period defined as the number of years in which the yearly perception is expected to return. It is the proportional estimation of the probability when expressed as a fraction:

$$T_X = \frac{1}{P_X}$$

3.2. Hydrology model

Digital Elevation Model, derived from Aster DEM having 30m spatial resolution and for Land cover data, Landsat 8 having 30m spatial resolution was used. Other data like rainfall data from Chennai Metrological Department and Soil type map from Water Resources Department were used in the study. A general flowchart of the hydrology model is shown in Figure 3.

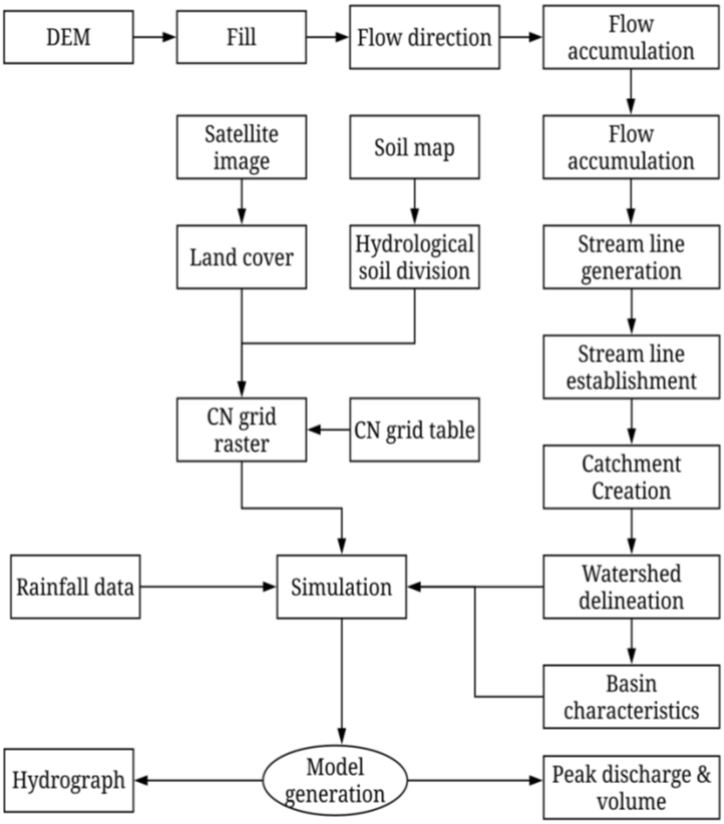

Figure 3: Flowchart of model generation

The Adyar basin covers an area of 830.7 sq.km, which is too large for a manual survey. So, the product HEC-GeoHMS is an extension used in the ArcGIS environment for the delineation of the watershed and developing other characteristics (Fleming & Doan, 2009). An Aster GDEM has been utilized for the analysis. The 'run and fill' command was utilized to fill-up the depressions. The 'flow direction' raster was created out of 'fill raster'. After that point, the 'flow direction' raster was processed to get 'flow accumulation' raster. The 'flow accumulation' setup depicts the stream way of the river profile in a raster form. Utilising 'flow accumulation' raster, the streamlines are extracted out of the 'flow accumulation' raster. Following this, the 'stream link' raster was created from the 'stream' raster and was further segregated into divisions. Stream links are the segments of a stream, which interface two progressive intersections and an outlet point. By determining an outlet point in 'stream link' raster, the entire basin was isolated into different sub-basins. By this procedure of converting raster to vector, a number of polygons were created and each stream was generated as a polyline. Then, the abutting drainage region was connected to outlet points. The adjoining basins produced using the different stream, are not the tributary of this waterway. The outlet point was marked using project point and the AOI (Area of Interest) was demarcated from all other basins (Mandal & Chakrabarty, 2016).

Sub-basin division: Coefficient of runoff is a vital parameter for drainage area behavior and runoff generation. Drainage area was associated at various time periods and the dampening impact on precipitation of different regions was sensed (Garambois, Larnier, Roux, Labat, & Dartus, 2014). Based on the number of streams, the model has delineated 11 sub-basins. In order to make the analysis simple, the sub-basins were merged into four main sub-basins namely Thirusoolam, Orathur, Dasarikuppam, and Manimagalam.

Characteristics of Basin: To evaluate the hydrograph, the behavior and other attributes of the basins are important. The precipitation inconstancy across the region assumes a noteworthy part when precipitation values are methodically organized across areas with the same amount of flow distance coordinates (Wu, Hsu, Lien, & Chang, 2015). The slope is also an important parameter, which is ascertained from the Digital Elevation Model. Each pixel value depicts the Z-axis value (height) of the particular region. For example, every pixel's X and Y will be constant because of the 30-m resolution of the DEM data, the only variable is the Z value (say 15). Therefore, the formula to calculate is

$$\tan(\theta) = \frac{opposite}{adjacent}$$

That is

$\theta = \tan^{-1}\frac{15}{30}$= 26° 33' 54.184"

Similarly, the slope for each pixel was calculated to generate the slope map, which was very helpful in the generation of river and basin slope. Basin centroid and longest flow path are also the important parameters that were calculated based on the previous output and the Aster GDEM.

Classification of Hydrological soil group: The computation of the Curve Number (CN), require to arrange the soils of the particular area according to their runoff capacity. These were classified as hydrological soil groups (Table 2).

Table 2: Hydrological soil division

Soil group	Infiltration	Rate (mm/hr)
A	High	7.6
B	Moderate	3.8 to 7.6
C	Flat	1.27 to 3.8
D	Very low	0 to 1.27

Source: (SCS, 1972)

Land cover: The land cover was associated with the soil group for the runoff curve number. Land cover of Chennai was created using Landsat 8 TM by unsupervised classification method. In a multispectral image, each and every pixel on the image has a digital number which assigns them to a spectral signature. Unsupervised classification will extract data from the multispectral image that is to assign the pixels to classes depending on their similar spectral signatures. For instance, the greater part of the pixels that represent a zone of built-up area on a TM raster ought to have generally the same spectral signature (F.Sabins, n.d.). Classification methods attempt to organize the similar

pixels and assign it to the designated class. Then, on the GIS layer, each class was given a separate color code for each land cover type. Unsupervised classification is a strategy in which the program sorts the relative pixel into a group known as a cluster. In ERDAS imagine, 'unsupervised classification' has been carried out utilizing an algorithm known as the Iterative Self-Organizing Data Analysis Technique (ISODATA). With the help of this algorithm, the number of clusters and a confidence threshold was fed in. Following this, the program processed the clusters iteratively, intending that with every distinct emphasis, the clusters end up being progressively refined. The cycles ended when the confidence level (or the most extreme number of emphases were reached as entered) was obtained (R. Jensen, 1996).

Table 3: Classes and its description

Classes	Description
Water	River, open water, lakes, ponds and reservoirs
Agriculture	Crop fields
Wasteland	Vacant land
Built-up area	Residential, commercial, industrial, transportation, roads, mixed urban
Forest land	Mixed forest land

In this study, 100 clusters were used at 95% Confidence interval. Once the clusters were assembled, the number of land cover classes were determined (water, agricultural land, Wasteland, Build-up area and forest), at that point each class was assigned to the desired classes. Table 3 shows the classes and its description, which were to be grouped under the same head.

CN grid generation: The performance of the Curve Number-precipitation function was examined deductively, and it corresponds to the alterations in natural landscape noted in the real world watershed (Soulis & Valiantzas, 2012). The land cover classes and the hydrological soil group were combined to generate the CN grid raster (Table 4, Figure 4).

Table 4: Runoff curve number from the Indian condition

Land cover	CN			
	A	B	C	D
Water	100	100	100	100
Agricultural land	59	69	76	79
Wasteland	71	80	85	88
Built up area	77	86	91	93
Forest	26	40	58	61

Source: (Kumar, N TIWART, & Pal, 1991)

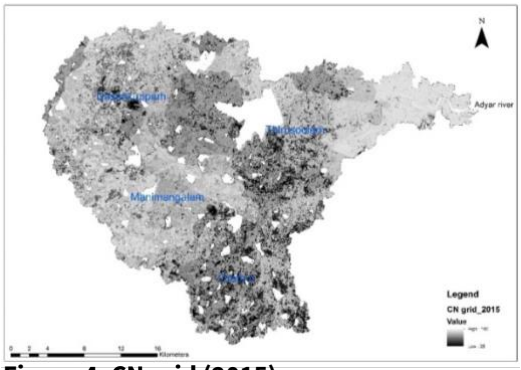

Figure 4: CN grid (2015)

From the CN grid raster, qualities of the watershed and the drainage pattern, and different characteristics were added to the attributes of the centroid. At last, the model was exported to HMS software for further processing.

HMS: HEC-HMS is a rainfall-runoff model created by the U.S. Army Corps of Engineers (USACE), Hydrologic Engineering Center. It intends to mimic the occasional and continuous rainfall-runoff process of dendritic watershed frameworks (Feldman, 2000). Jang et al., 2007 expressed that the *Disaster Impact Assessment Manual*, 2005 proposes the utilization of engineered hydrograph systems, for example, the Storm Water Management Model (SWMM) is valuable when the zone has streamflow data while the Soil Conservation Service (SCS) technique is used when there is a lack of streamflow data due to the absence of hydrological station. Therefore the Soil Conservation Service method was adopted for this study as: (1) It is basically used in various conditions and still yields a good outcome (2) computation process is less demanding and requires few variables like hydrologic soil group, land use data and slope for evaluation; and (3) in spite of its simplicity, it's yields are in the same class as of sophisticated models(Lastra, Fernández, Díez-Herrero, & Marquínez, 2008).

Soil Conservation Service *(SCS) Loss method:* This module in HEC-HMS modelling environment computes the amount of precipitation which ultimately turns into runoff. This model includes the connection between the land cover, hydrologic soil class, and curve number. Typically the SCS method processes runoff is calculated using the following equation(Bansode & Patil, 2014):

$$P_E = \frac{(P - I_A)^2}{(P + 0.8 * S)}$$

Where, P_E = Excess precipitation, P = Accumulated rainfall, S = Potential maximum retention [S = (25400/CN) – 254] and I_A =Initial abstraction (0.2 * S)

Composite CN is calculated from the following expression:

$$CN_{composite} = \frac{\sum(Area_i * CN_i)}{Total\ Area_i}$$

Where, CN = Curve number, CN=30 (very permeable) and CN=100 (Impervious layer)

SCS Unit Hydrograph model: It is a recognized, ordinarily utilized strategy for relating precipitation abundance to direct runoff. Sherman initially proposed the Unit Hydrograph in 1932 expressing, "… the basin surge because of one unit of direct runoff produced consistently over the drainage area at a uniform precipitation rate amid a predefined time of precipitation duration"(Feldman, 2000). The runoff generation framework was supposed to be linear, so the runoff from greater or lesser than one unit was basically a multiple of the unit hydrograph (Feldman, 2000). In HEC-HMS the Unit Hydrograph was computed using the equation:

$$Q_n = \sum_{m=1}^{n \le M} P_m U_{n-m+1}$$

where: Q_n is storm hydrograph ordinate at time nΔt (m^3/s), P_m is rainfall excess depth in time interval mΔt to (m+1)Δt (mm) and $U_{n-m+1}$is Unit Hydrograph ordinate at the time (n-m+1). It has dimensions of flow rate per unit depth.

The Soil Conservation Service Unit Hydrograph technique is a parametric Unit Hydrograph generation method. This implies that the Unit Hydrograph ordinates are ascertained over an arrangement of equations after the parameters of the equations are indicated. The center of this model is a dimensionless, single-peaked Unit Hydrograph. The dimensionless Unit Hydrograph states the discharge, U_t as a proportion of discharge to the Unit Hydrograph peak discharge, U_P for any time t and a fraction of the T_P, the time to Unit Hydrograph peak (Feldman, 2000). The relationship amongst U_P and T_P are

$$U_P = C\frac{A}{T_P}$$

where: A is watershed area and C is conversion constant.

The time to peak has a relationship with the unit of rainfall excess as

$$T_P = \frac{\Delta t}{2} + t_{lag}$$

where: Δt is the excess rainfall duration and t_{lag} is the basin lag.

HEC-HMS solves the relationship amongst U_P and T_P to bring out the height of the Unit Hydrograph peak and also compute time to peak relationship to the unit of rainfall excess to bring out the time of Unit Hydrograph peak. The basin lag time is the main contribution of this method. The basin lag time is computed for every watershed in view of the time of concentration (t_c).

$$t_{lag} = 0.6\, t_c$$

The primary values of t_c are assessed utilizing HEC-GeoHMS extension and the TR-55 flow path segment tool. Utilizing this tool, breakpoints were distinguished along the longest flow path to isolate the areas for different types of flow like sheet flow, shallow concentrated flow and channel flow(Feldman, 2000).

Muskingum-Cunge routing method: In hydrological methods, the continuity is expressed by equating the difference between inflow and outflow to the rate of change of storage in the reach as:

$$Q_i - Q_o = \frac{ds}{dt}$$

The Muskingum method uses a storage equation, which is linear in its form and is given by :

$$S = k\{\varepsilon Q + (1-\varepsilon)Q\}$$

where: k is storage coefficient and ε is a dimensionless factor that defines the relative weights of inflow and outflow. The Muskingum-Cunge technique is similar to the Muskingum technique. It utilises a deliberate cross-section and channel properties to decide the routing coefficients. Karmegam, 1981 built up the work on parameter estimation for flood routing and was later researched by Rangapathy, V., Karmegam, M. and Sakthivadive (1988) to determine k and ε which identify the physical attributes utilizing:

$$k = \Delta x / V_w$$

where: Δ x is reach length (m) and V_w is the average speed of the flood wave (m/s).

$$\varepsilon = 1/2(1-(Q/\Delta x V_w B S_o))$$

where: B = top width (m) and S_o = slope

The simulation was run for the month of November and December, 2015 with the daily precipitation data. The result of the simulation showed the hydrograph and the volume of the water. Through this, the peak time and the peak discharge were determined.

3.3. Hydraulic Modelling

HEC-RAS is an integrated system of software. The framework is inclusive of Graphical User Interface, separate hydraulic analysis components, data storage and management capabilities, graphics and reporting facilities(W.Brunner, 2016).

Customarily, 1D river models have been utilized to show fluvial flooding occasions. 1D models are comprised of a progression of cross sections depicting the geography of the waterway. Furthermore, floodplain and water levels are figured utilizing the 1-D form of the represented conditions. 1D models just require topographic information to be gathered at the cross section that makes up the model, which is a preferred standpoint when access to

topographic information is constrained. While 1-Dimensional models perform well when the flow is confined between channel banks, 2-Dimensional modeling has appeared to better estimate flows in geographically complex floodplains, where the flow is accounted generally in 2-dimensions (V. Tayefi, S. N. Lane, 2010), (Vojinovic & Tutulic, 2009). Coupled 1D-2D models, simulates channel flow utilizing a 1D approach, and overbank flow is modeled in 2D. The 1D model is run independently to create a boundary condition to the 2D area of the model, this is alluded to as loose coupling, and this approach has been used in a number of studies (Mcmillan & Brasington, 2007) & (D. Yu & Lane, 2011).

Dapeng Yu, 2005 compared the loose coupling method and a tight coupling method, where the 1-Dimensional and 2-Dimensional areas are linked on a time step basis. The examination demonstrated that the decision of the coupling system could affect modeled inundation extent. Moreover, they demonstrated that loose coupling could result in progressive errors since water cannot flow once again into the 1-Dimensional area of the model. Tight 1D-2D couplings are frequently computed utilizing lateral weir conditions, where the flow is ascertained from the WLD (Water Level Difference). Late investigations by Morales-Hernández, Petaccia, Brufau, & García-Navarro, 2016 have suggested 1D-2D coupling strategies where both mass and momentum is moderated. The adaptation of HEC-RAS utilized as a part of this study considers 1D-2D coupling on a time-step basis. The flow between the spaces can be ascertained utilizing a lateral weir condition (W.Brunner, 2016) and on the other hand by forcing 1D water levels onto the 2D area as a stage boundary condition(W.Brunner, 2016). The tight 1D-2D model was chosen for this study. Unsteady fluid flow changes with both space and time. The unsteady fluid flow is represented by the conservation of mass and energy, which can be depicted by a set of equations known as the St.Venant equation.

1D unsteady flow: In numerous river-modeling applications, it is accepted that the flow is 1D. It is computed utilizing the 1D equation of the St.Venant which is,

1D Continuity equation: The continuity equation portrays the preservation of mass in a defined control volume. It calculates the net mass flux which equals the change in storage. The 1D type of the St.Venant continuity condition can be composed in the accompanying structure:

$$\frac{\partial Q}{\partial x} + \frac{\partial A}{\partial t} + q = 0$$

Where Q is the flow rate, A is the cross-sectional area and q is the lateral inflow.

1D momentum equation-This equation depends on Newton's second law of motion, defining that total force acting on a given element will be equal to the rate of change of momentum. The creation of the equation depends on the

kind of forces that are taken into account. By considering the pressure, gravity and frictional resistance as the factors, the 1D continuity equation is represented as:

$$\frac{\partial V}{\partial t} + g\frac{\partial}{\partial x}\left(\frac{V^2}{2g} + h\right) = g(S_0 - S_f)$$

Where V is the flow velocity, g is the gravitational acceleration, h is the water depth, S_0 is the bed slope and S_f is the friction slope.

2D Unsteady flow: When contemplating flow over complex floodplains the presumption that flow is 1D may no longer be substantial. 2D unsteady flow shifts in time and along two spatial measurements. The overseeing standards of 2D unsteady flow are the same with respect to 1D flow, the conservation of mass and momentum.

2D continuity equation- This is very similar to the 1D equation. The net mass flux into the designated volume is equal to the change in storage in the control volume. The difference is that the mass fluxes are now calculated in 2D using the following expression:

$$\frac{\partial H}{\partial t} + \frac{\partial (hu)}{\partial x} + \frac{\partial (hv)}{\partial y} + q = 0$$

Where H is the water surface elevation, h is the water depth, u and v are the depth-averaged velocities in the x- and y-direction, and q is the source term, representing inflow from external sources such as precipitation. (Chaudhry, 2008).

2D momentum equation: As in the 1D case, the momentum balance is based on the principle that the sum of forces acting on an element equals the rate of change of momentum. Considering forcing from gravity, eddy viscosity (momentum exchange), friction and the Coriolis effect, the 2D momentum balance equations can be written as follows: Momentum balance in the x-direction:

$$\frac{\partial u}{\partial t} + u\frac{\partial u}{\partial x} + v\frac{\partial u}{\partial y} = -g\frac{\partial H}{\partial x} + v_t\left(\frac{\partial^2 u}{\partial x^2} + \frac{\partial^2 u}{\partial y}\right) - c_f$$

The momentum balance in the y-direction:

$$\frac{\partial u}{\partial t} + u\frac{\partial u}{\partial x} + v\frac{\partial u}{\partial y} = -g\frac{\partial H}{\partial x} + v_t\left(\frac{\partial^2 u}{\partial x^2} + \frac{\partial^2 u}{\partial y^2}\right) - c_f u + fv$$

where H is the water surface elevation, v_t is the eddy viscosity coefficient, c_f is the friction coefficient, f is the Coriolis parameter and v and u are depth-averaged velocities in the x and y directions respectively (Brunner, 2016). Using the Manning's formula, the friction coefficient c_f can be expressed as following (in the x-direction):

$$c_f = \frac{n^2 g|u|}{R^{\frac{4}{3}}}$$

where n is Manning's n value, g, the gravitational constant, u, the velocity in the x-direction and R, the hydraulic radius.

4.RESULTS

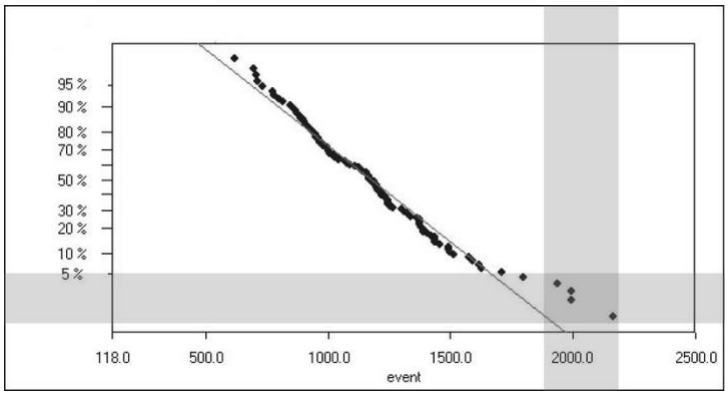

Figure 5: Probability of exceedance

4.1 Rainfall analysis: The probability of exceedance was calculated for the 115-year rainfall through CDF (Figure 5). It was found that the 2015 event (1992 mm) had less than 5% probability. The return period of the 2015 flooding event (1992 mm) is predicted to be 124 years.

4.2. Land cover change detection

The land cover of 2005 and 2015 was processed through Landsat 8 images (30m cell size) using supervised classification.

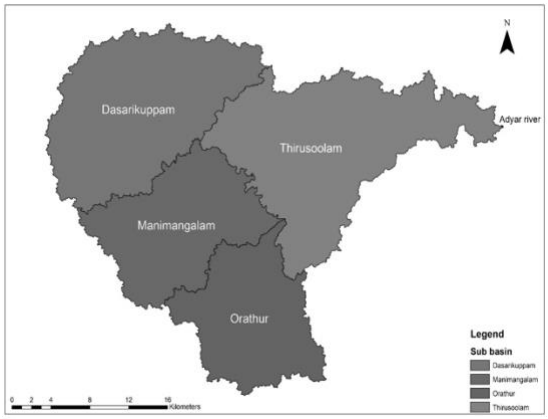

Figure 6: Adyar watershed with its sub-basin

The delineated watershed falls under 4C2C2 watershed code according to AISLUS, 1990. The 2005 land cover for the Adyar watershed has 7.6% of water, 27.3% of the agricultural land, 20.1% of wasteland, 28.9% of Built-up area and 16.1% of the forest. While 2015 land cover for the Adyar watershed (Figure 6) has 7.8% of water, 32.8% of the agricultural land, 3.7% of the wasteland, 44.4% of the built-up area and 11.4% of the forest. Comparison matrix was built between 2005 and 2015 to compare the land cover change. There is a tremendous change in the built-up area

from 28.9% to 44.4%. Land cover in 2015 has been deprived of 69.9 sq.km of agricultural land, 55.9 sq.km of wastelands and 10.1 sq.km of forest area to add up to the built-up area. This has played a vital role in worsening the situation.

4.3. Generation of scenarios: HMS model was simulated for two different scenarios to understand the characteristics of the parameter which influenced the entire system.

2015 Scenario: It was generated using land use map, rainfall and reservoir data of 2015 as input. The four sub-basins namely Orathur, Manimangalam, Dasarikuppam, Thirusoolam have the peak discharge of 614.8, 687.7, 994.9, 1129.3 m^3/sec respectively. At the estuary point, maximum discharge of 2947.6 m^3/sec was noted. The hydrograph for the 2015 scenario is shown in Figure 7.

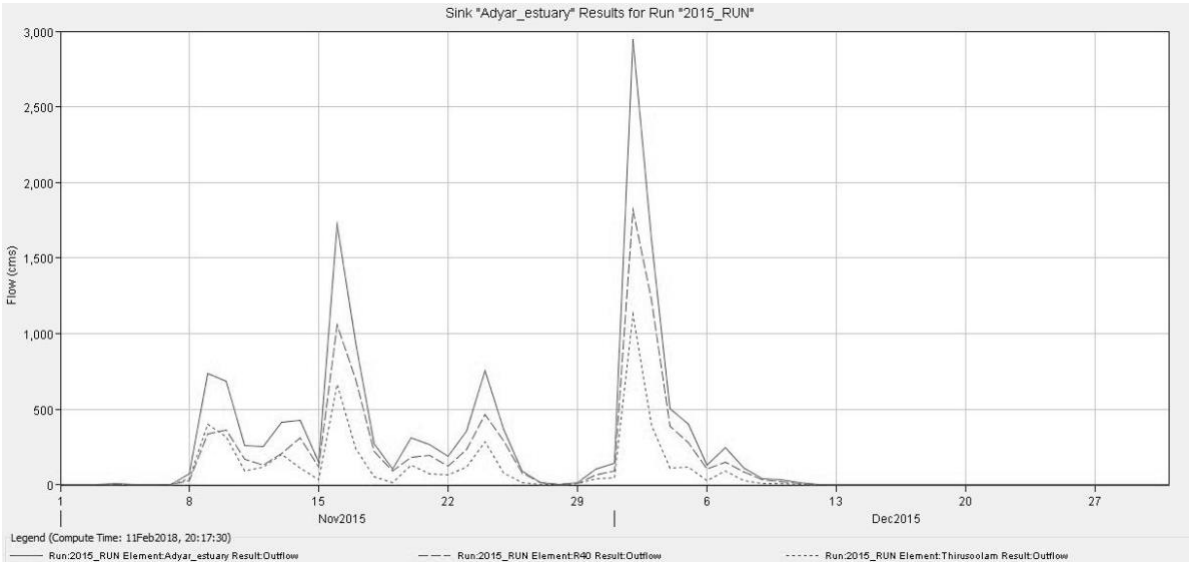

Figure 7: Hydrograph for 2015 flood event

2005 scenario: It was generated by adding in land use map, rainfall and reservoir discharge data for 2005 as input. The results showed that the, four sub-basins namely Orathur, Manimangalam, Dasarikuppam, Thirusoolam have peak discharge of 352.2, 403.7, 582.1, 659.2 m^3/sec respectively. At the estuary point, maximum discharge of 1608.8 m^3/sec was noted. The hydrograph for the 2005 scenario is shown in Figure 8.

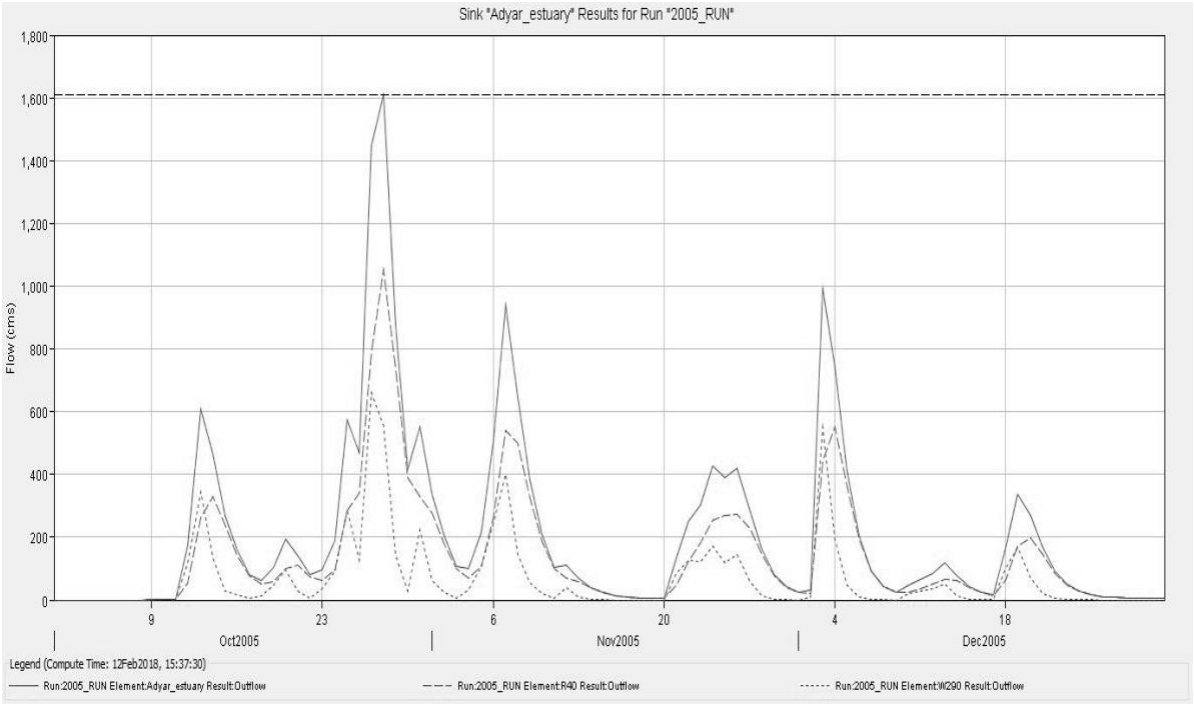

Figure 8: Hydrograph for 2005 flood event

With 2005 CN grid and the rainfall and reservoir discharge data of 2015: It was generated with the help of the land use map of 2005, and rainfall, and reservoir data of 2015 as input. By running a simulation using this dataset, the computed results showed that the four sub-basins namely Orathur, Manimangalam, Dasarikuppam, Thirusoolam have the peak discharge of 611.7, 686.8, 993.1, 1126.3 m^3/sec respectively. At the estuary point, maximum discharge of 2582.6 m^3/sec was noted. There was a difference of 12.4% in peak discharge of 2015. Hence, we can conclude that the land cover change inflated the peak discharge.

2005 CN grid but rainfall data of 2015: 2005 scenario was generated by inserting a 2005 land use map, 2005 reservoir data, and 2015 rainfall. Similarly, the four sub-basins namely Orathur, Manimangalam, Dasarikuppam, Thirusoolam have the peak discharge of 611.7, 686.8, 993.1, 1126.3 m^3/sec respectively. At the estuary point, maximum discharge of 2240.6 m^3/sec was noted. There was a difference of 23.9% in peak discharge of 2015. The summary of all the generated scenarios is shown in table 5. From the table, it is evident that the land cover change and the poor reservoir management created the huge impact in the peak discharge.

Table 5: Generated scenarios

Scenarios	Peak discharge (m^3/sec) at estuary	Difference from 2015
2015	2947	
2005	1608	1337 (45.4%)
2005 CN grid (change in rainfall and reservoir discharge data-2015)	2582	365 (12.4%)
2005 CN grid (Change in rainfall data-2015)	2240	707 (23.9%)

Hydraulic modeling: The physical attributes of the river channels, cross-sections (creating and assigning n values) and other hydraulic structures were computed using HEC-GeoRAS. After pre-processing, the data was exported to the HEC-RAS for further processing.

4.4. HEC-RAS*:* Every RAS layer was imported into the geometric window and the spatial reference was input in '.prj' format. The 2D mesh was generated for the study area and the Manning's n value was assigned to the formulated grid. Thereafter, the flow data and boundary condition were assigned. Flows were regularly characterized at the start of the upstream area of every waterway/tributary, and at intersections. The discharge data with respect to the time was gathered from the hydrology model. 1D modeling flow data for the river channel (Adyar) and 2D modeling with precipitation data for the floodplains (CMA) were utilized.

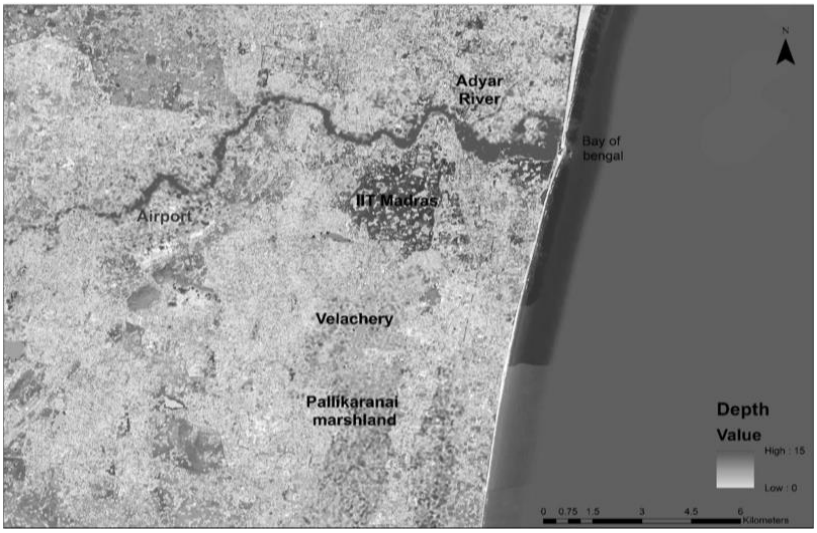

Figure 9: Flood inundation map

Running the model: The unsteady flow analysis was simulated for the run with the total flow data for the time frame (November to December'15). The cycle duration for computation was set according to the input given in the HEC-HMS. In this study, computation was

done hourly and finally the flood inundation map (Figure 9) was obtained.

5. RECOMMENDATION:

Flood risk mitigation is a long-term and ongoing process, prior to the occurrence of a disaster that is directed at reducing future flood damages of the community and the nation ("FEMA," 2010). Generally, there is no flood risk that cannot be mitigated through engineering measures, but the cost seems to be the determining factor. In this study, the following location-based flood risk reduction strategies have been suggested for preventive mitigation. The non-engineering measures- Warning systems and Regulations and the engineering measures- Improvement of channels and creation of infiltration basin are explained further.

5.1 Non-Engineering measures: Real-time flood forecasting systems depend upon the hydrological, hydraulic model and other hydro-informatics tool to portray the complicated models into a simple format for the decision makers to devise the strategies to implement (Martina, Todini, & Libralon, 2005). After creating scenarios by running the complex hydraulic and hydrological model, the warning systems and future predictions become more effective. Some of the suggested location-specific risk reduction measures are shown in table 6.

Table 6: Mitigation and Flood Risk Reduction Measures suggested for Chennai

Measures	Problem	Solution
Flood warning system	Lack of graphical information for the decision makers to act according. (Sung, Tsai, & Kang, n.d.)	A statutory body should be created and this should have access to the flood modelling and management related data
Strom water management	There should be a location specific drainage design standard	Optimum return period should be chosen by adding climate change also as a factor
Norms for building roads and material	Inappropriate usage of material and construction techniques.	N.O.C should be made mandatory from the statutory body for any real-estate modification or development
Maintenance of drainage system	Disposal of waste into the river channel(Lamond, Bhattacharya, & Bloch, 2012).	Declaring strict punishments or monetary penalties for disposal of waste into the channel. Inspection office A (City) and B (outside the city) should be built for regular supervision

2035 scenario generation: Future urban growth scenario using strategies such as High Rise and High Density (HRHD)or Low Rise and High Density (LRHD) has been studied for the Chennai region based on growth projections for the year 2035, with respect to flood has been further studied (figure 10).

The same procedure discussed earlier has been applied to carry out the simulation for both high-rise and high density and low-rise and high-density development. The results are shown in table 7 which clearly indicates that the Adyar watershed should follow HRHD trend.

Table 7: 2035 scenarios

2035	Peak discharge (m^3/sec) at estuary	Newly affected area	Newly affected population
High rise and high density	3174	8.9 sq.km	2.6 Lakhs
Low rise and high density	3541	22.9 sq.km	6.8 Lakhs

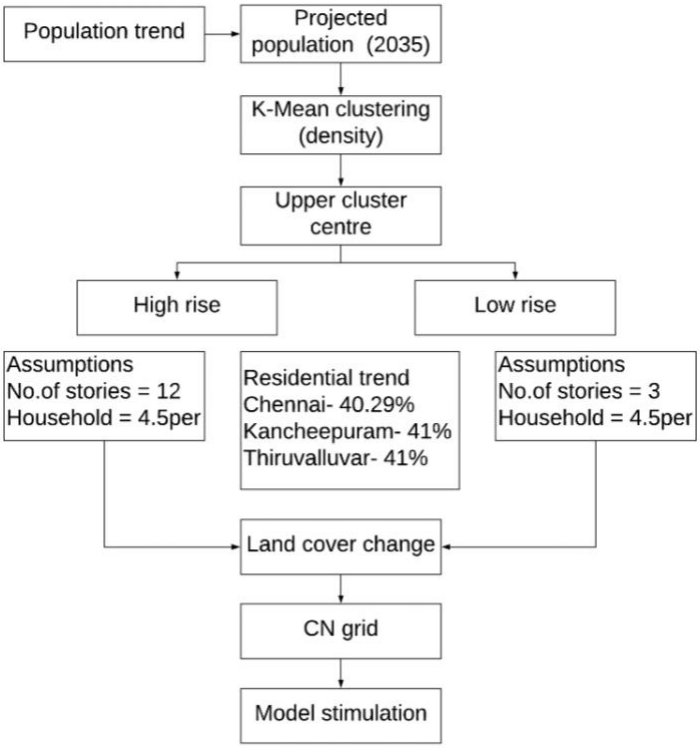

Figure 10: Methodology for future scenario (2035)

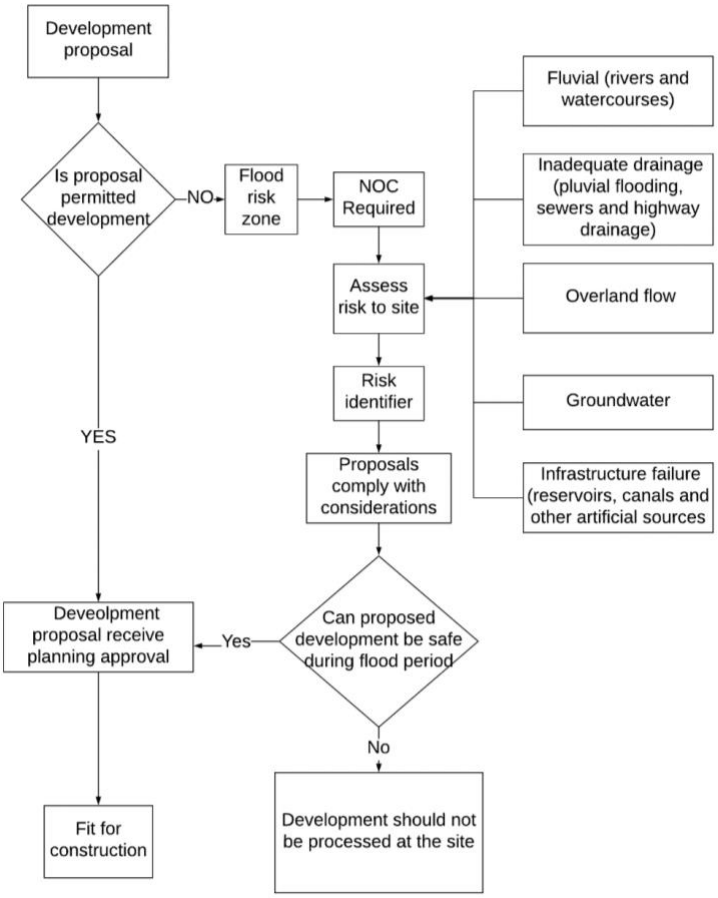

Figure 11: Urban Flood Disaster Risk Reduction Decision-Making Methodology

Typical site approval: This involves locating any new development in areas having lower flood risk. Every new development should mandatorily acquire an N.O.C (No Objection Certificate) from the Government authority so as not impede the flow of the natural drainage. The flowchart depicts the urban flood disaster risk reduction strategy that would assess a site through various stages of verification (Figure 11). From the model, flood depth of the particular area is known. By having this as the base, the area-specific bye-laws can be created. The building should be constructed with respect to their flood depth in the particular area. Perforated compound wall should be created in order to allow the hydrological flow to pass through. Rainwater harvesting and pond should be created for increasing the infiltration of rainwater into the ground. This will reduce the load in the channel and also helps in recharging the groundwater.

5.2. Engineering measures: *River mouth dredging- Phase I (Figure 12):*

The distance for each chainage length is marked from the tip of the mouth of the river to the end of the river (Figure 13). At the estuary point, there is the formation of sandbars. The sandbars should be removed for effective channel flow into the sea (Table 8).

Table 8: Excavation phase I

	Area (Approx.) m^2	Height (Approx.) m	Volume (Approx.) (cu.m)	Construction Sand (Approx.) (cu.m)
A	85456	3.3	282005	85456
B	22430	3.3	74019	22430
C	64825	5	324125	-
D	26989	3.3	89064	-
E	20911	3	62733	-
Total			8,31,946	1,07,886

Figure 13: Locations for dredging river at mouth

Figure 12: Adyar river- chainage in metre

Some parts of excavated sand consist of usable sand and the rest should be laid over the bunds or used for beach nourishment.

Channel dredging- Phase II: The main objective is to minimize the desilting volume and optimizing hydraulic improvement for 124-year return period flood design (Table 9).

Table 9: Excavation phase II

From	To	Proposed width of the river to be desilted (m)	Proposed depth of the river to be desilted (m)	Volume to be excavated (Cu.m)
2000	3000	200	2	3,98,500
3000	4000	200	1.8	3,58,500
4000	5000	100	1.6	1,58,500
5000	6000	60	1.4	82,500
6000	7000	60	1.4	82,500
7000	8000	60	1.2	70,500
8000	9000	60	1.2	70,500
9000	10000	30	0.5	13,500
10000	11000	40	0.6	22,500
11000	12000	30	0.7	19,500
Total				12,77,000

This is done through an iterative process. The center of the channel should be widened for the chainage lengths suggested for effective control against recurrent urban floods (Figure 14, 15).

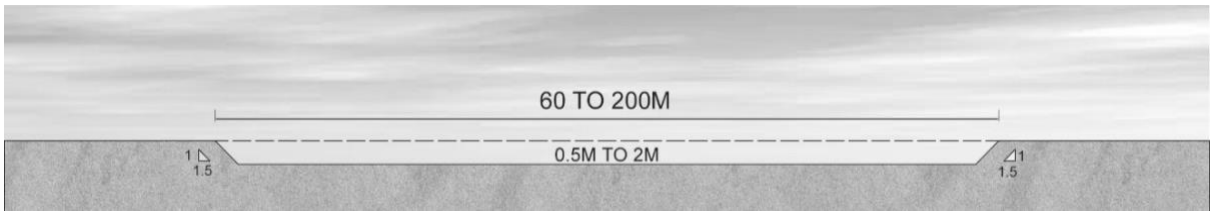

Figure 14: Chainage- 2000m to 8000m (200 to 300m wide)

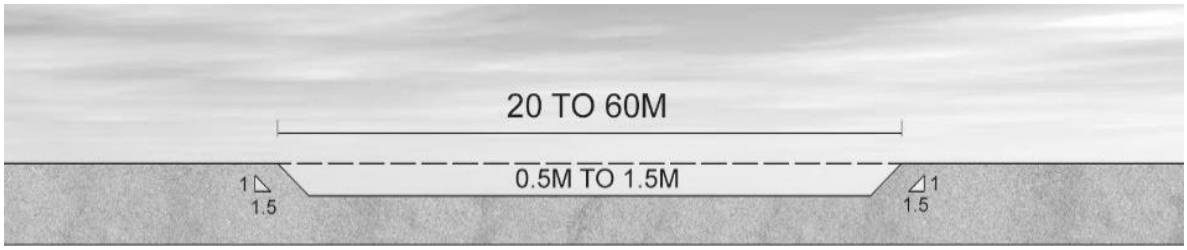

Figure 15: Chainage- 8000m to 11,000 km

Proposal for construction of a swale:

Swales are channels which are shallow and used to gather and move water while managing any contamination in the surface water. The profile relies on the following variables: ground levels, topography, ground and soil conditions, orientation, aspect and proximity and other landscape features, buildings etc. Specific areas have been suggested as a disaster risk reduction strategy considering slope and flow direction, land availability, Entisols (soil type- since as it has the highest infiltration rate), surrounded by forest or wasteland. The locations have been marked as A - 4.6 sq.km, B- 2.05 sq.km, C- 2.7 sq.km, D- 2.24 sq.km (Approx.) (Figure 16). The volume of water on the event day was 65701 x 10^3 cu.m. After engineering measures, the volume of water was reduced by swale through infiltration into the soil was 8344 x 10^3 cu.m. /day, excavation during phase 1 is 831 x 10^3 cu.m. and phase 2 is 1277 x 10^3 cu.m.. Hence, there was a total reduction of 10453 x 10^3 cu.m. in the volume of water, which amounts to 15.9% reduction of the total volume of water on the event day.

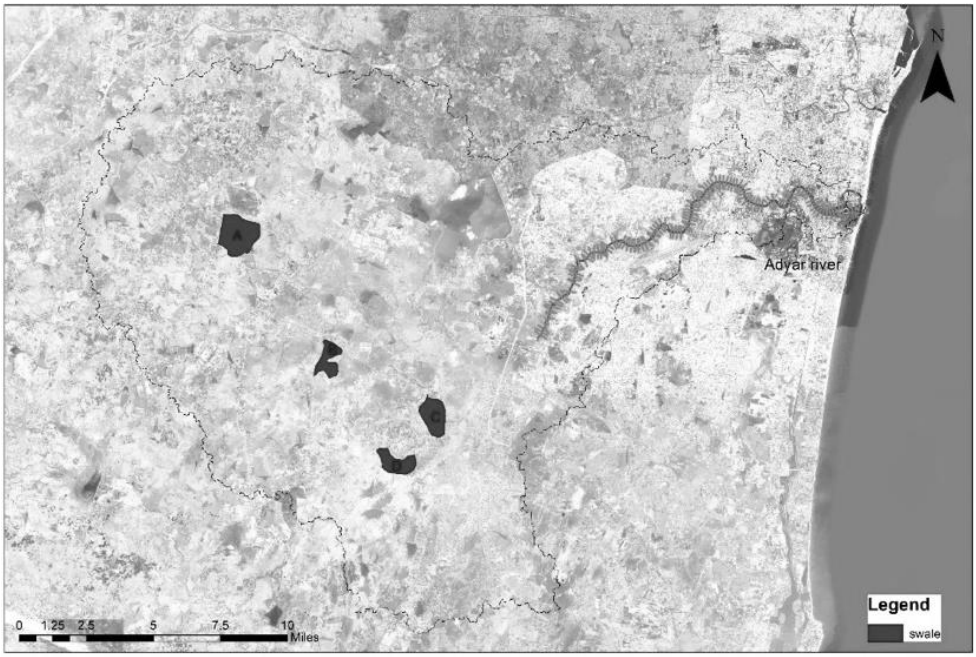

Figure 16: Location of proposed swale

6.CONCLUSION

This study suggests a methodology for risk reduction strategy for urban flood which has been implemented in Chennai, India. The above-mentioned recommendations could prove to be effective and each of the suggested remedial measure provides scope for further exploration individually. The simulation results from this study could establish the effectiveness of both engineering and non-engineering measures. It is essential that primary focus is given to both the types of measures but, the non-engineering measures need to be strengthened and revised with respect to time.

For any city region, hydrological and hydraulic simulation of the flood event before and after adoption of risk reduction measures can be studied and the effectiveness of both engineering and non-engineering solutions can be ascertained. A cost benefit assessment of the options available would optimize the choice of control measures. Furthermore, a high level of adaptability is required with respect to land-use planning and management is necessary in developing countries that are witnessing large scale growth of urban areas. Mitigation of urban flood and risk reduction strategies involves an integrated web of engineering, non-engineering measures, and policy actions for the safety of its residents.

References

Bansode, A., & Patil, K. A. (2014). Estimation of Runoff by using SCS Curve Number Method and Arc GIS. *International Journal of Scientific & Engineering Research*, *5*(7). Retrieved from http://www.ijser.org

Curebal, I., Efe, R., Ozdemir, H., Soykan, A., & Sönmez, S. (2016). GIS-based approach for flood analysis: case study of Keçidere flash flood event (Turkey). *Geocarto International*, *31*(4), 355–366. https://doi.org/10.1080/10106049.2015.1047411

Disaster Impact Assessment Manual. (2005). South Korea.

F.Sabins, F. (n.d.). *Remote sensing: Principles and Interpretation* (3rd ed.).

Feldman, A. D. (2000). *Hydrologic modelling system HEC-HMS: technical reference manual*. US Army Corps of Engineers, Hydrologic Engineering Center.

FEMA. (2010). Retrieved May 31, 2018, from https://www.fema.gov/what-mitigation#

Fleming, M. J., & Doan, J. H. (2009). HEC-GeoHMS Geospatial Hydrologic Modelling Extension User's Manual. Retrieved from http://www.hec.usace.army.mil/software/hec-geohms/documentation/HEC-GeoHMS_Users_Manual_4.2.pdf

Garambois, P. A., Larnier, K., Roux, H., Labat, D., & Dartus, D. (2014). Analysis of flash flood-triggering rainfall for a process-oriented hydrological model. *Atmospheric Research*, *137*, 14–24. https://doi.org/10.1016/J.ATMOSRES.2013.09.016

Haan, C. T. (1986). *Statistical Methods in Hydrology*. The Iowa State University Press / Ames.

Hannah Ritchie and Max Roser. (2017). OFDA/CRED International Disaster Data - Our World in Data. Retrieved May 14, 2018, from https://ourworldindata.org/ofdacred-international-disaster-data

Hernandez, T., & Zhang, B. (n.d.). FLOODPLAIN ANALYSIS USING COMPUTATIONAL TOOLS. Retrieved from http://www.ltrr.arizona.edu/~katie/kt/FLOODS-USGS/NSF-AHIS/World-Env-Water-Res-Congress-Proc-2007/40927-3378.pdf

Jang, S., Cho, M., Yoon, J., Yoon, Y., Kim, S., Kim, G., … Aksoy, H. (2007). Using SWMM as a tool for hydrologic impact assessment. *Desalination*, *212*(212), 344–356. https://doi.org/10.1016/j

Karmegam. (1981). *Parameter Identification in Flood Routing*. University of London.

Kumar, P., N TIWART, K., & Pal, D. (1991). *Establishing SCS runoff curve number from IRS digital database*. *Journal of the Indian Society of Remote Sensing* (Vol. 19). https://doi.org/10.1007/BF03023971

Lamond, J., Bhattacharya, N., & Bloch, R. (2012). The role of solid waste management as a response to urban

flood risk in developing countries, a case study analysis (pp. 193–204). https://doi.org/10.2495/FRIAR120161

Lastra, J., Fernández, E., Díez-Herrero, A., & Marquínez, J. (2008). Flood hazard delineation combining geomorphological and hydrological methods: an example in the Northern Iberian Peninsula. *Natural Hazards*, *45*(2), 277–293. https://doi.org/10.1007/s11069-007-9164-8

LKS Pvt. India. (2012). *Chennai River Restoration Trust report*. Chennai.

Mandal, S. P., & Chakrabarty, A. (2016). Flash flood risk assessment for upper Teesta river basin: using the hydrological modelling system (HEC-HMS) software. *Modelling Earth Systems and Environment*, *2*(2), 59. https://doi.org/10.1007/s40808-016-0110-1

Martina, M. L. V., Todini, E., & Libralon, A. (2005). A Bayesian decision approach to rainfall thresholds based flood warning. *Hydrology and Earth System Sciences Discussions*, *2*(6), 2663–2706. https://doi.org/10.5194/hessd-2-2663-2005

Mcmillan, H., & Brasington, J. (2007). *Reduced complexity strategies for modelling urban floodplain inundation*. *Geomorphology* (Vol. 90). https://doi.org/10.1016/j.geomorph.2006.10.031

Morales-Hernández, M., Petaccia, G., Brufau, P., & García-Navarro, P. (2016). Conservative 1D-2D coupled numerical strategies applied to river flooding: The Tiber (Rome). *Applied Mathematical Modelling*, *40*(3), 2087–2105. https://doi.org/10.1016/j.apm.2015.08.016

Ohl, C. A., & Tapsell, S. (2000). Flooding and human health : The dangers posed are not always obvious. *BMJ : British Medical Journal*, *321*(7270), 1167–1168. Retrieved from http://www.ncbi.nlm.nih.gov/pmc/articles/PMC1118941/

Price, R. K., & Vojinovic, Z. (n.d.). CASE STUDY Urban flood disaster management. https://doi.org/10.1080/15730620802099721

R. Jensen, J. (1996). *Introductory Digital Image Processing: A Remote Sensing Prospective*. *SERBIULA (sistema Librum 2.0)*.

Rangapathy, V., Karmegam, M. and Sakthivadive1, R. (1988). A monograph on Flood Routing Methods as Applied to Indian Rivers. *Anna University Publication*.

SCS. (1972). *SCS national engineering handbook, section 4: hydrology*. The Service. Retrieved from https://books.google.co.in/books?id=sjOEf-5zjXgC

Smith, K., & Ward, R. (1998). *Floods: Physical processes and human impacts*. Chichester, USA: John wiley and

sons.

Snead, D. B. (2000). Development and Application of Unsteady Flood Models Using Geographic Information Systems. Retrieved from https://repositories.lib.utexas.edu/bitstream/handle/2152/6827/crwr_onlinereport00-12.pdf?sequence

Soulis, K. X., & Valiantzas, J. D. (2012). SCS-CN parameter determination using rainfall-runoff data in heterogeneous watersheds – the two-CN system approach. *Hydrology and Earth System Sciences*, *16*(3), 1001–1015. https://doi.org/10.5194/hess-16-1001-2012

Sung, E.-X., Tsai, M.-H., & Kang, S.-C. (n.d.). FloodViz: A Visual-Based Decision Support System for Flood Hazard Warning. Retrieved from https://pdfs.semanticscholar.org/dfbb/4dfad50fd2e5b28082b7670294b14900a228.pdf

UN-SPIDER Knowledge Portal. (n.d.). Retrieved May 14, 2018, from http://www.un-spider.org/risks-and-disasters/natural-hazards/flood

V. Tayefi, S. N. Lane, R. J. H. and D. Y. (2010). A comparison of one- and two-dimensional approaches to modelling flood inundation over complex upland floodplain. *HYDROLOGICAL PROCESSES*, *21*, 3190–3202. https://doi.org/10.1002/hyp

Vojinovic, Z., & Tutulic, D. (2009). On the use of 1D and coupled 1D-2D modelling approaches for assessment of flood damage in urban areas. *Urban Water Journal*, *6*(3), 183–199. https://doi.org/10.1080/15730620802566877

W.Brunner, G. (2016). US Army Corps of Engineers HEC-RAS River Analysis System Hydraulic Reference Manual. Retrieved from http://www.hec.usace.army.mil/software/hec-ras/documentation/HEC-RAS 5.0 Reference Manual.pdf

Wiitala, S. W., Sommerville, A. J., Jetter, K. R., & Pennsylvania. (1961). Hydraulic and hydrologic aspects of flood-plain planning. Washington, D.C.: U.S. G.P.O. Retrieved from file://catalog.hathitrust.org/Record/101738208

Works, C. S. D. of P. (1923). *Flow in California streams*.

Wu, S.-J., Hsu, C.-T., Lien, H.-C., & Chang, C.-H. (2015). Modelling the effect of uncertainties in rainfall characteristics on flash flood warning based on rainfall thresholds. *Natural Hazards*, *75*(2), 1677–1711. https://doi.org/10.1007/s11069-014-1390-2

Yu, D. (2005). Diffusion-based modelling of flood inundation over complex floodplains.

Yu, D., & Lane, S. N. (2011). Interactions between subgrid-scale resolution, feature representation and grid-scale resolution in flood inundation modelling. *Hydrological Processes*, *25*(1), 36–53. https://doi.org/10.1002/hyp.7813